DELFT UNIVERSITY OF TECHNOLOGY

REPORT 19-03

Point Forces and Their Alternatives in Cell-Based Models for Skin Contraction

Q. Peng, F.J. Vermolen

ISSN 1389-6520

Reports of the Delft Institute of Applied Mathematics

Delft 2019

Point Forces and Their Alternatives in Cell-Based Models for Skin Contraction

Q.Peng, F.J.Vermolen

Oct, 2019

Abstract

During wound healing, contractions occur due to the pulling forces released by (myo)fibroblasts. We consider a cell-based approach in which the balance of momentum is used to predict the cellular impact on the mechanics of the tissue. To this extent, the elasticity equation and Dirac Delta distributions are combined. However, Dirac Delta distributions cause a singular solution. Hence, alternative approaches are developed and a Gaussian distribution is often used as a smoothed approach. Based on the application that the pulling force is pointing inward the cell, the smoothed particle approach is probed as well. In one dimension, it turns out that the aforementioned three approaches are consistent. In fact, we are aware that the similar transformation exists in three dimensional electric dipole moment. For two dimensions, the ratio of the force magnitude is only worked out in special case, but for the general case, the numerical results show consistency between the direct approach and the smoothed particle approach.

1 Introduction

Wound healing is the spontaneous process of the skin to cure itself after an injury. It is a complex cascade of cellular events which contribute to resurfacing, reconstitution and restoration of the tensile strength of injured skin. For severe traumas, due to a significant loss of soft tissue, dermal wounds may lead to various pathological problems like contractures, which are known as excessive and morbid contractions. Usually, contractures concur with disfunctioning and disabilities of the patients.

Generally speaking, there are four overlapping phases in wound healing: hemostasis, inflammation, proliferation and maturation/remodelling. The contractions of the wound appear from the third phase of wound healing, which usually starts from the second day and will continue for two to four weeks after wounding[3]. During proliferation, epithelialization, fibroplasia, angiogenesis and the development of granulation tissue are included. After epithelialization, repairing of injured dermis commences. The blood clot, which is develop in the hemostasis to prevent more blood lost and seal off the wound from its surroundings, is broken by proteins and gradually replaced by granulation tissue, which consists of various cells and connective tissues[1]. Fibroblasts are attracted to the wound area from the uninjured region by a number of factors like platelet-derived growth factor (PDGF) and transforming growth factor-beta(TGF-beta)[3]. Once within the wound, fibroblasts mostly differentiate into myofibroblats which pull the extracellular matrix even more hardly and causing wound deformation[2, 4, 7].

In summary, wound contractions take place due to (myo)fibroblasts interacting with the environment, namely the extracellular matrix(ECM) and the formation of (permanent) stresses and strain by collagen distributions in and around the wound area. In other words, the contractions are developed by the (myo)fibroblasts exerting pulling forces on the skin. In the

end, usually, the contractions will result in $5-10\%$ reduction from the original volume of the wound[3]. Notably, contraction must be distinguished from contracture, which is a pathological process of excessive contraction and caused by the application of excessive stress to the wound.

According to Koppenol et al. [5], the forces released by the (myo)fibroblasts can be categorized as temporary forces and permanent forces. Only temporary forces will be discussed in this paper, of which the formalization is developed by Vermolen and Gefen [8]. In the model, the elasticity equation and Dirac Delta distributions are incorporated. However, Dirac Delta distributions cause a singular solution, that is, for dimensionality exceeding one the solution is not in the same Hilbert space as the basis functions for many naive finite-element strategies. In order to circumvent this complication, the smoothed forces approach is developed, in which we use Gaussian distributions to replace Dirac Delta distributions. Especially in our healing model, the forces point towards the centre of the cell. Therefore, we use the gradient of Gaussian distribution as an alternative.

The boundary value problems for all three methods are displayed in Section 2 for both one and two dimensions. Section 3 shows the numerical results corresponding to the approaches investigated before. In Section 4, conclusions are delivered.

2 Mathematical Models

To describe the contraction of the tissue we use the equation for conservation of momentum over the computational domain Ω:

$$-\nabla\cdot\boldsymbol{\sigma}=\boldsymbol{f}. \tag{2.1}$$

In the above equation, inertia has been neglected. We consider a linear, homogeneous, isotropic material; hence, Hooke's Law is used here to define $\boldsymbol{\sigma}$ for dimensionality exceeding one:

$$\boldsymbol{\sigma}=\frac{E}{1+\nu}\left\{\boldsymbol{\epsilon}+tr(\boldsymbol{\epsilon})\left[\frac{\nu}{1-2\nu}\right]\boldsymbol{I}\right\}, \tag{2.2}$$

where E is the stiffness of the computational domain, ν is Poisson's ratio and $\boldsymbol{\epsilon}$ is the infinitesimal strain tensor:

$$\boldsymbol{\epsilon}=\frac{1}{2}\left[\boldsymbol{\nabla u}+(\boldsymbol{\nabla u})^T\right]. \tag{2.3}$$

The forces exerted by a cell are modelled by Dirac Delta distributions on the midpoints of the segments of the boundary of the cell[8]; hereby, we only consider one relatively big cell in the computational domain:

$$\boldsymbol{f}_t = \sum_{j=1}^{N_S^i} P(\boldsymbol{x},t)\boldsymbol{n}(\boldsymbol{x})\delta(\boldsymbol{x}-\boldsymbol{x}_j^i(t))\Delta\Gamma_N^{i,j} \tag{2.4}$$

$$\rightarrow \int_{\partial\Omega_N^i} P(\boldsymbol{x},t)\boldsymbol{n}(\boldsymbol{x})\delta(\boldsymbol{x}-\boldsymbol{x}_s^i(t))d\Gamma_N^i, \quad \text{as } N_S^i\rightarrow\infty, \tag{2.5}$$

where N_S^i is the number of line segments of cell i, $P(\boldsymbol{x},t)$ is the magnitude of the pulling force exerted at point $\boldsymbol{x}$ and time t per length, $\boldsymbol{n(x)}$ is the unit inward pointing normal vector (towards the cell centre) at position $\boldsymbol{x}$, $\boldsymbol{x}_j^i(t)$ is the midpoint on line segment j of cell i at time t and $\Delta\Gamma_N^{i,j}$ is the length of line segment j. In Eq (2.5), $\boldsymbol{x}_s^i(t)$ represents a point on the cell boundary of cell i at time t.

2.1 Elasticity Equation and Point Sources in One Dimension

Considering the force equilibrium in one dimension, the equations are expressed as

$$\begin{aligned} -\frac{d\sigma}{dx} &= f, && \text{Equation of Equlibirum,} && (2.6)\\ \epsilon &= \tfrac{du}{dx}, && \text{Strain-Displacement Relation,} && (2.7)\\ \sigma &= E\epsilon, && \text{Constitutive Equation.} && (2.8) \end{aligned}$$

To simplify the equation with $E = 1$ here, the equations above can be combined to Laplacian equation in one dimension:

$$-\frac{d^2u}{dx^2} = f. \tag{2.9}$$

2.1.1 With Dirichlet Boundary Condition

According to Eq (2.4), for one dimension, assume there is a cell with size h and centre position c in the computational domain $(0, L)$. Combined with homogeneous Dirichlet boundary conditions, the boundary value problem of the direct approach is given by

$$(BVP_\delta)\begin{cases} -\dfrac{d^2u}{dx^2} = \delta(x-(c+\dfrac{h}{2})) - \delta(x-(c-\dfrac{h}{2})), \quad x \in (0,L),\\ u(0) = u(L) = 0, \end{cases} \tag{2.10}$$

where $\delta(x-x')$ is Dirac Delta distribution. Note that in one dimension, the solution is piecewise linear and hence in $H^1(\Omega)$.

The Gaussian distribution is usually used as a replacement for Dirac Delta distributions to obtain a smoother expression. Here, we denote

$$\delta_\varepsilon(x-x') = \frac{1}{\sqrt{2\pi\varepsilon^2}} \exp\left\{-\frac{(x-x')^2}{2\varepsilon^2}\right\}$$

for the Gaussian distribution with mean x' and variance ε^2. Therefore, the boundary value problem of the smoothed approach is expressed as

$$(BVP_S)\begin{cases} -\dfrac{d^2u_\varepsilon}{dx^2} = \delta_\varepsilon(x-(c+\dfrac{h}{2})) - \delta_\varepsilon(x-(c-\dfrac{h}{2})), \quad x \in (0,L),\\ u_\varepsilon(0) = u_\varepsilon(L) = 0, \end{cases} \tag{2.11}$$

In (BVP_s), since the right-hand side is smooth, we can rewrite it as

$$\begin{aligned} &\delta_\varepsilon(x-(c+\frac{h}{2})) - \delta_\varepsilon(x-(c-\frac{h}{2})) = h\frac{d\delta_\varepsilon}{dx}(x-c+\eta)\\ &\Rightarrow \frac{1}{h}(\delta_\varepsilon(x-(c-\frac{h}{2})) - \delta_\varepsilon(x-(c+\frac{h}{2}))) = \frac{d\delta_\varepsilon}{dx}(x-c+\eta), \quad \exists\eta \in (-\frac{h}{2},\frac{h}{2}). \end{aligned} \tag{2.12}$$

As $h \to 0$, Eq (2.12) turns into

$$\lim_{h\to 0}\frac{1}{h}(\delta_\varepsilon(x-(c-\frac{h}{2})) - \delta_\varepsilon(x-(c+\frac{h}{2})) = \frac{d\delta_\varepsilon}{dx}(x-c). \tag{2.13}$$

In other words, the right hand side of (BVP_S) converges to right-hand side of the smoothed particle approach:

$$(BVP_{SP})\begin{cases} -\dfrac{d^2v_\varepsilon}{dx^2} = h\dfrac{d\delta_\varepsilon}{dx}(x-c), \quad x \in (0,L),\\ v_\varepsilon(0) = v_\varepsilon(L) = 0, \end{cases} \tag{2.14}$$

as $h \to 0$. This, in turn is combined with the boundary conditions to conclude that the difference between u_ϵ and v_ϵ satisfies a homogeneous Laplace equation as $h \to 0$, and hence $v_\epsilon \to u_\epsilon$ as $h \to 0$. In fact, we are aware that in electric dipole moment, especially in three dimensional case of potential forum, there are similar transformations occurring in potential expression of an electric dipole. Taylor expansion is applied to bridge the potential expression of two points charge transferring to one point charge expressed with gradient; see Laud [6] for more details.

Hereby, we will prove the convergence of the solutions of (BVP_S) and (BVP_{SP}) with applying Poincaré's inequality and Taylor's expansion.

Lemma 2.1. (Poincaré's Inequality) *For any function $\boldsymbol{u}$ in the Sobolev space, and a given bounded domain Ω, such that $\boldsymbol{u} = \mathbf{0}$ on the boundary of Ω, there exits a constant C such that*

$$\|\boldsymbol{u}\|_{L^p(\Omega)} \leqslant C\|\nabla \boldsymbol{u}\|_{L^p(\Omega)}, \tag{2.15}$$

where $1 \leqslant p < \infty$.

Theorem 2.1. *Denote u_ε and v_ε as the solutions to the boundary value problems (BVP_S) and (BVP_{SP}) respectively in one dimension with Dirichlet boundary condition, then as the length of the cell h turns to zero, $v_\varepsilon \to u_\varepsilon$.*

Proof. We consider $w_\varepsilon = u_\varepsilon - v_\varepsilon$ and subtract Eq (2.11) and Eq (2.14), a new boundary value problem of w_ε is expressed as

$$\begin{cases} -\dfrac{d^2 w_\varepsilon}{dx^2} = \delta_\varepsilon(x - (c - \dfrac{h}{2})) - \delta_\varepsilon(x - (c + \dfrac{h}{2})) - h\dfrac{d\delta_\varepsilon}{dx}(x - c), \quad x \in (0, L), \\ w_\varepsilon(0) = w_\varepsilon(L) = 0. \end{cases} \tag{2.16}$$

By Taylor expansion and there exits $(\eta_1, \eta_2) \in (0, 1)$, such that the above equations become

$$\begin{cases} -\dfrac{d^2 w_\varepsilon}{dx^2} = \dfrac{h^3}{48}\left[\delta_\varepsilon^{(3)}(x - (c - \dfrac{h}{2}\eta_1)) + \delta_\varepsilon^{(3)}(x - (c - \dfrac{h}{2}\eta_2))\right], \quad x \in (0, L), \\ w_\varepsilon(0) = w_\varepsilon(L) = 0. \end{cases} \tag{2.17}$$

Here, $\delta_\epsilon^{(3)}$ is the third derivative of Gaussian distribution with variance ε. Note that

$$\left\|\frac{h^3}{48}\left[\delta_\varepsilon^{(3)}(x - (c - \frac{h}{2}\eta_1)) + \delta_\varepsilon^{(3)}(x - (c - \frac{h}{2}\eta_2))\right]\right\| \leqslant \frac{h^3}{48} \times 2 \times \|\delta_\varepsilon^{(3)}\| = \frac{h^3}{24} \times \|\delta_\varepsilon^{(3)}\|.$$

Then we multiply $w_\epsilon(x)$ on both sides and taking integral over $(0, L)$, and it gives

$$\begin{aligned} &-\int_0^L w_\varepsilon''(x) w_\varepsilon(x) dx \leqslant \frac{h^3}{48} \times 2\|\delta_\epsilon^{(3)}\| \int_0^L w_\varepsilon''(x) dx \\ &\Rightarrow -\left[w_\varepsilon'(x) w_\varepsilon(x)\right]_0^L + \int_0^L (w_\varepsilon'(x))^2 dx \leqslant \frac{h^3}{24} \times \|\delta_\epsilon^{(3)}\| \int_0^L w_\varepsilon''(x) dx \\ &\Rightarrow w_\varepsilon^2(L) + w_\varepsilon^2(0) + \int_0^L (w_\varepsilon'(x))^2 dx \leqslant \frac{h^3}{24}\|\delta_\epsilon^{(3)}\| L \|w_\varepsilon(x)\|_{L^2((0,L))} \\ &\Rightarrow \int_0^L (w_\varepsilon'(x))^2 dx \leqslant \frac{h^3}{24}\|\delta_\epsilon^{(3)}\| L \|w_\varepsilon(x)\|_{L^2((0,L))}. \end{aligned}$$

Combined with Poincaré's inequality (see Lemma 2.1), we can obtain that there exists a positive constant K, such that

$$\|w_\varepsilon\|_{L^2((0,L))} \leqslant L\frac{h^3}{24K} \times \|\delta_\varepsilon^{(3)}\|.$$

Hence, $\|w_\varepsilon\| \to 0$, as $h \to 0$, which implies the convergence between u_ε and v_ε. □

For the direct approach, the exact solution is the linear combination of the Green' function in one dimension, which is known as

$$G(x,x') = \begin{cases} x'(1-\dfrac{x}{L}), & x \geqslant x', \\ x(1-\dfrac{x'}{L}), & x < x'. \end{cases} \tag{2.18}$$

Since the forces are inward pointing to the centre of the cell, the solution to (BVP_δ) is

$$u_\delta(x) = G(x, c-\frac{h}{2}) - G(x, c+\frac{h}{2}). \tag{2.19}$$

The solutions to (BVP_S) and (BVP_{SP}), are, respectively, given by

$$\begin{aligned} u_{S_\varepsilon}(x) = &\frac{x\varepsilon}{\sqrt{2}L}\left(\int_{-\frac{c-h/2}{\sqrt{2}\varepsilon}}^{\frac{L-(c-h/2)}{\sqrt{2}\varepsilon}} \operatorname{erf}(x')dx' - \int_{-\frac{c+h/2}{\sqrt{2}\varepsilon}}^{\frac{L-(c+h/2)}{\sqrt{2}\varepsilon}} \operatorname{erf}(x')dx'\right) \\ &- \frac{\varepsilon}{\sqrt{2}}\left(\int_{-\frac{c-h/2}{\sqrt{2}\varepsilon}}^{\frac{x-(c-h/2)}{\sqrt{2}\varepsilon}} \operatorname{erf}(x')dx' - \int_{-\frac{c+h/2}{\sqrt{2}\varepsilon}}^{\frac{x-(c+h/2)}{\sqrt{2}\varepsilon}} \operatorname{erf}(x')dx'\right), \end{aligned} \tag{2.20}$$

and

$$u_{SP_\varepsilon}(x) = \frac{h}{2}\left\{(\frac{x}{L}-1)\operatorname{erf}(\frac{c}{\sqrt{2}\varepsilon}) + \frac{x}{L}\operatorname{erf}(\frac{L-c}{\sqrt{2}\varepsilon}) - \operatorname{erf}(\frac{x-c}{\sqrt{2}\varepsilon})\right\}, \tag{2.21}$$

where $\operatorname{erf}(x)$ is the error function defined as $\operatorname{erf}(x) = \frac{2}{\sqrt{\pi}}\int_0^x \exp(-t^2)dt$.

2.1.2 With Robin's Boundary Conditions

We consider the same partial differential equations stated in Eq (2.7), (2.8) and (2.7) with the following Robin's boundary condition:

$$-u'(0) + u(0) = 0, -u'(L) + u(L) = 0,$$

for one dimensional domain $(0, L)$. Following the same assumptions before, there is a cell with size h and centre position c, then the boundary value problem of the direct approach is given by

$$(BVP_\delta)\begin{cases} -\dfrac{d^2u}{dx^2} = \delta(x-(c+\dfrac{h}{2})) - \delta(x-(c-\dfrac{h}{2})), \quad x \in (0,L), \\ -u'(0) + u(0) = 0, \\ -u'(L) + u(L) = 0. \end{cases} \tag{2.22}$$

The solution is

$$u_\delta(x) = -\frac{1+x}{2+L}h + (x-(c-\frac{h}{2}))_+ + (x-(c+\frac{h}{2}))_+, \tag{2.23}$$

where $(x)_+ = \max\{0, x\}$. Substituting $x = 0$, Eq (2.23) delivers $u(0) = -\frac{h}{2+L}$. For the smoothed approach, using Gaussian distribution as an approximation of Dirac Delta distribution, the boundary value problem is expressed as

$$(BVP_S)\begin{cases} -\dfrac{d^2u_\varepsilon}{dx^2} = \delta_\varepsilon(x-(c+\dfrac{h}{2})) - \delta_\varepsilon(x-(c-\dfrac{h}{2})), \quad x \in (0,L), \\ -u'_\varepsilon(0) + u_\varepsilon(0) = 0, \\ -u'_\varepsilon(L) + u_\varepsilon(L) = 0. \end{cases} \tag{2.24}$$

The solution to this is

$$u_{S_\varepsilon}(x) = \frac{\mathcal{G}'_{\varepsilon,c+h/2}(L) + \mathcal{G}_{\varepsilon,c+h/2}(L)}{2+L}(1+x) - \mathcal{G}_{\varepsilon,c+h/2}(x) - \frac{\mathcal{G}'_{\varepsilon,c-h/2}(L) + \mathcal{G}_{\varepsilon,c-h/2}(L)}{2+L}(1+x) + \mathcal{G}_{\varepsilon,c-h/2}(x), \tag{2.25}$$

where $\mathcal{G}_{\varepsilon,c}(x) = \int_0^x \int_0^s \delta_\varepsilon(t-c)dtds$. Substituting $x = 0$, we obtain

$$u_{S_\varepsilon}(0) = \frac{(\mathcal{G}'_{\varepsilon,c+h/2}(L) + \mathcal{G}_{\varepsilon,c+h/2}(L)) - (\mathcal{G}'_{\varepsilon,c-h/2}(L) + \mathcal{G}_{\varepsilon,c-h/2}(L))}{2+L}.$$

As $\varepsilon \to 0$, $\delta_\varepsilon(x)$ tends to $\delta(x)$, therefore,

$$\lim_{\varepsilon\to 0} \mathcal{G}'_{\varepsilon,c}(x) = \lim_{\varepsilon\to 0} \int_0^x \delta_\varepsilon(t-c)dt = H(s-c), \tag{2.26}$$

$$\lim_{\varepsilon\to 0} \mathcal{G}_{\varepsilon,c}(x) = \lim_{\varepsilon\to 0} \int_0^x \int_0^s \delta_\varepsilon(t-c)dtds = \int_0^x H(s-c)ds = (x-c)_+, \tag{2.27}$$

where $H(x)$ is Heaviside step function, defined as the integral of the Dirac Delta distributions. We notice that $u_\delta \to u_{S_\varepsilon}$ when ε goes to zero. Combining Eq (2.26) and (2.27) with $x = L$ and $c - h/2, c + h/2 \in (0, L)$, it gives

$$\begin{cases} \lim\limits_{\varepsilon\to 0} \mathcal{G}'_{\varepsilon,c+h/2}(L) = \lim\limits_{\varepsilon\to 0} \mathcal{G}'_{\varepsilon,c-h/2}(L) = 1, \\ \lim\limits_{\varepsilon\to 0} \mathcal{G}_{\varepsilon,c+h/2}(L) = L - (c+h/2), \\ \lim\limits_{\varepsilon\to 0} \mathcal{G}_{\varepsilon,c-h/2}(L) = L - (c-h/2). \end{cases}$$

Thus,

$$\lim_{\varepsilon\to 0} u_{S_\varepsilon}(0) = -\frac{h}{2+L} = u_\delta.$$

To prove u_{S_ε} converges to u_δ as $\varepsilon \to 0$, we apply Eq (2.26) and (2.27), then

$$\begin{aligned} u_{S_\varepsilon}(x) &\to \frac{1+L-(c+h/2)}{2+L}(1+x) - (x-(c+h/2))_+ \\ &\quad - \frac{1+L-(c-h/2)}{2+L}(1+x) + (x-(c-h/2))_+ \\ &= -\frac{h}{2+L}(1+x) - (x-(c+h/2))_+ + (x-(c-h/2))_+ \\ &= u_\delta(x), \quad \text{as } \varepsilon \to 0 \text{ and for all } x \in (0,L). \end{aligned}$$

Next, we consider the smoothed particle approach with Robin's boundary condition, that is

$$(BVP_{SP}) \begin{cases} -\dfrac{d^2 v_\varepsilon}{dx^2} = h\dfrac{d\delta_\varepsilon}{dx}(x-c), \quad x \in (0,L), \\ -v'_\varepsilon(0) + v_\varepsilon(0) = 0, \\ -v'_\varepsilon(L) + v_\varepsilon(L) = 0. \end{cases} \tag{2.28}$$

The solution to it is given by

$$\begin{aligned} u_{SP_\varepsilon}(x) = \frac{h}{2+L} &\left(\frac{1}{4\sqrt{\pi}\varepsilon^2} \exp\{-\frac{(L-c)^2}{2\varepsilon^2}\} + \frac{1}{2}\operatorname{erf}(\frac{L-c}{\sqrt{2}\varepsilon}) + \frac{1}{2}\operatorname{erf}(\frac{c}{\sqrt{2}\varepsilon}) \right. \\ &\left. - \frac{1}{\sqrt{2\pi\varepsilon^2}}(1+L)\exp\{-\frac{c^2}{2\varepsilon^2}\} \right)(1+x) + hx\frac{1}{2\pi\varepsilon^2}\exp\{-\frac{c^2}{2\varepsilon^2}\} \\ &- \frac{h}{2}\left(\operatorname{erf}(\frac{L-c}{\sqrt{2}\varepsilon}) + \operatorname{erf}(\frac{c}{\sqrt{2}\varepsilon}) \right) \end{aligned} \tag{2.29}$$

Lemma 2.2. (Friedrich's Inequality) *For an open bounded domain $\Omega \subset \mathbb{R}^n$ with boundary $\partial\Omega$, there exists a positive constant C, such that for any function $u \in H^1(\Omega)$,*

$$\int_\Omega u^2 d\Omega \leqslant C\left[\int_\Omega \|\nabla u\|^2 d\Omega + \int_{\partial\Omega} u^2 d\Omega\right]$$

Theorem 2.2. *Denote u_ε and v_ε as the solutions to the boundary value problems (BVP_S) and (BVP_{SP}) respectively in one dimension with Robin's boundary condition, then as the length of the cell h turns to zero, $v_\varepsilon \to u_\varepsilon$.*

Proof. To prove the convergence between the solutions of u_{S_ε} and u_{SP_ε}, we will use Taylor expansion and define $w_\varepsilon = u_\varepsilon - v_\varepsilon$ in Eq (2.24) and (2.28) respectively, then we obtain the boundary value problem for w_ε

$$\begin{cases} -\dfrac{d^2 w_\varepsilon}{dx^2} = \dfrac{h^3}{48}\left[\delta_\varepsilon^{(3)}(x-(c-\dfrac{h}{2}\eta_1)) + \delta_\varepsilon^{(3)}(x-(c-\dfrac{h}{2}\eta_2))\right], \quad x \in (0,L), \\ -w_\varepsilon'(0) + w_\varepsilon(0) = 0, \\ -w_\varepsilon'(L) + w_\varepsilon(L) = 0, \end{cases} \tag{2.30}$$

where there exits $(\eta_1, \eta_2) \in (0,1)$. Multiplying $w_\varepsilon(x)$ on both sides and taking the integral over the domain $(0, L)$, it gives

$$\begin{aligned} &-\int_0^L w_\varepsilon''(x) w_\varepsilon(x) dx = \int_0^L \frac{h^3}{48}\left[\delta_\varepsilon^{(3)}(x-(c-\frac{h}{2}\eta_1)) + \delta_\varepsilon^{(3)}(x-(c-\frac{h}{2}\eta_2))\right] w_\varepsilon''(x) dx \\ &\Rightarrow -\left[w_\varepsilon'(x) w_\varepsilon(x)\right]_0^L + \int_0^L (w_\varepsilon'(x))^2 dx \leqslant \frac{h^3}{48} \times 2\|\delta_\epsilon^{(3)}\| \int_0^L w_\varepsilon''(x) dx \\ &\Rightarrow w_\varepsilon^2(L) + w_\varepsilon^2(0) + \int_0^L (w_\varepsilon'(x))^2 dx \leqslant \frac{h^3}{24}\|\delta_\epsilon^{(3)}\| L \|w_\varepsilon(x)\|_{L^2((0,L))}. \end{aligned}$$

Applying Friedrich's inequality (see Lemma 2.2), there exists $K > 0$, such that

$$\begin{aligned} &K\|w_\varepsilon(x)\|_{L^2((0,L))}^2 \leqslant w_\varepsilon^2(L) + w_\varepsilon^2(0) + \int_0^L w_\varepsilon'(x) dx \leqslant \frac{h^3}{24}\|\delta_\epsilon^{(3)}\| L \|w_\varepsilon(x)\|_{L^2((0,L))} \\ &\Rightarrow |w_\varepsilon(x)\|_{L^2((0,L))} \leqslant \frac{h^3 L}{24K}\|\delta_\epsilon^{(3)}\| \to 0, \text{as } h \to 0. \end{aligned}$$

Hence, we proved that $v_\varepsilon \to u_\varepsilon$. □

2.2 Elasticity Equation and Point Sources in Two Dimensions

For two dimensions, we start with analysing only one cell in the computational domain. According to the model described in Eq (2.4), the forces released on the boundary of the cell are the superposition of point forces on the midpoint of each line segment. For example, if we use a square shape to approximate the cell, then the forces are depicted in Figure 2.1. Therefore, in this circumstance, the forces can be rewritten as

$$\begin{aligned} \boldsymbol{f}_t &= P\left\{\begin{bmatrix}1\\0\end{bmatrix}\Delta y \delta(x-(a+\frac{\Delta x}{2}), y-b) - \begin{bmatrix}1\\0\end{bmatrix}\Delta y \delta(x-(a-\frac{\Delta x}{2}), y-b)\right. \\ &\quad \left. + \begin{bmatrix}0\\1\end{bmatrix}\Delta x \delta(x-a, y-(b+\frac{\Delta y}{2})) - \begin{bmatrix}0\\1\end{bmatrix}\Delta x \delta(x-a, y-(b-\frac{\Delta y}{2}))\right\} \\ &\approx P\left\{\begin{bmatrix}1\\0\end{bmatrix}\Delta y\left[\delta_\varepsilon(x-(a+\frac{\Delta x}{2}), y-b) - \delta_\varepsilon(x-(a-\frac{\Delta x}{2}), y-b)\right]\right. \\ &\quad \left. + \begin{bmatrix}0\\1\end{bmatrix}\Delta x\left[\delta_\varepsilon(x-a, y-(b+\frac{\Delta y}{2})) - \delta_\varepsilon(x-a, y-(b-\frac{\Delta y}{2}))\right]\right\}. \end{aligned} \tag{2.31}$$

Thanks to the continuity of Gaussian distribution δ_ε, there exists $(\eta_x, \eta_y) \in (-\Delta x/2, \Delta x/2) \times (-\Delta y/2, \Delta y/2)$ such that, Eq (2.31) yields into

$$\begin{aligned} \boldsymbol{f}_t &\approx P\left\{ \begin{bmatrix} 1 \\ 0 \end{bmatrix} \Delta y \Delta x \frac{\partial \delta_\varepsilon}{\partial x}(x-a+\eta_x, y-b) + \begin{bmatrix} 0 \\ 1 \end{bmatrix} \Delta y \Delta x \frac{\partial \delta_\varepsilon}{\partial y}(x-a, y-b+\eta_y) \right\} \\ &\to P\Delta x \Delta y \nabla \delta_\varepsilon(x-a, y-b), \quad \text{as } \Delta x, \Delta y \to 0. \end{aligned} \tag{2.32}$$

The above procedure implies that as $\Delta x,\ \Delta y \to 0$, the right-hand side of the regularized Dirac Delta Distributions converges to $P\Delta x \Delta y \nabla \delta_\epsilon(x-a, y-b)$. This implies that the Laplacian of the difference between the solutions from both approaches converges to zero. Using the boundary conditions and the maximum principle for the Laplace equation, it implies that the difference between both approaches converges to zero pointwisely.

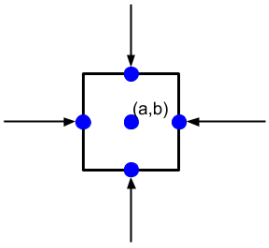

Figure 2.1: We consider a square shape cell, with the centre position at (a, b)***. The forces exerted on the boundary are indicated by arrows***

Theorem 2.3. *Let* $\boldsymbol{u_\varepsilon}$ *the solution to the boundary value problems*

$$(BVP_S) \begin{cases} -\nabla \cdot \boldsymbol{\sigma}(\boldsymbol{u}_\varepsilon) = P\left\{ \begin{bmatrix} 1 \\ 0 \end{bmatrix} \Delta y \Delta x \frac{\partial \delta_\varepsilon}{\partial x}(x-a+\eta_x, y-b) \right. \\ \qquad\qquad \left. + \begin{bmatrix} 0 \\ 1 \end{bmatrix} \Delta y \Delta x \frac{\partial \delta_\varepsilon}{\partial y}(x-a, y-b+\eta_y) \right\}, \boldsymbol{x} \in \Omega, \\ \qquad \boldsymbol{u_\varepsilon} = \boldsymbol{0}, \boldsymbol{x} \in \partial\Omega, \end{cases} \tag{2.33}$$

and $\boldsymbol{v_\varepsilon}$ *the solution to*

$$(BVP_{SP}) \begin{cases} -\nabla \cdot \boldsymbol{\sigma}(\boldsymbol{v}_\varepsilon) = P\Delta x \Delta y \nabla \delta_\varepsilon(x-a, y-b), \quad \boldsymbol{x} \in \Omega, \\ \qquad \boldsymbol{v_\varepsilon} = \boldsymbol{0}, \quad \boldsymbol{x} \in \partial\Omega. \end{cases} \tag{2.34}$$

As the size of the cell (i.e. $\Delta x, \Delta y$*) turns to zero,* $\boldsymbol{v_\varepsilon}$ *converges to* $\boldsymbol{u_\varepsilon}$*.*

Proof. Similarly, let $w_\varepsilon = u_\varepsilon - v_\varepsilon$, and subtract the equations above. There exists $(\eta_x, \eta_y) \in (0,1) \times (0,1)$, such that applying Taylor expansion, we obtain

$$\begin{cases} -\nabla \cdot \boldsymbol{\sigma}(\boldsymbol{w}_\varepsilon) = P\frac{1}{48}\Delta x^3 \Delta y \begin{bmatrix} 1 \\ 0 \end{bmatrix} \left[\frac{\partial^3 \delta_\varepsilon}{\partial x^3}(x-(a+\frac{h}{2}\eta_x), y-b) - \frac{\partial^3 \delta_\varepsilon}{\partial x^3}(x-(a-\frac{h}{2}\eta_x), y-b) \right] \\ \qquad\qquad + P\frac{1}{48}\Delta x \Delta y^3 \begin{bmatrix} 0 \\ 1 \end{bmatrix} \left[\frac{\partial^3 \delta_\varepsilon}{\partial y^3}(x-a, y-(b+\frac{h}{2}\eta_y)) - \frac{\partial^3 \delta_\varepsilon}{\partial y^3}(x-a, y-(b-\frac{h}{2}\eta_y)) \right], \boldsymbol{x} \in \Omega, \\ \qquad\qquad \boldsymbol{u_\varepsilon} = \boldsymbol{0}, \boldsymbol{x} \in \partial\Omega. \end{cases} \tag{2.35}$$

We multiply $w_\varepsilon(x)$ in both sides and take integral over the computational domain Ω. Due to the symmetry of strain tensor ϵ and the homogeneous boundary condition, $-\int_\Omega \nabla \cdot \boldsymbol{\sigma}(\boldsymbol{w}_\varepsilon)\boldsymbol{w}_\varepsilon d\Omega = \int_\Omega \boldsymbol{\sigma}(\boldsymbol{w}_\varepsilon) : \boldsymbol{\epsilon}(\boldsymbol{w}_\varepsilon) d\Omega$. Thus,

$$K \int_\Omega \boldsymbol{w}_\varepsilon^2 d\Omega \leqslant \int_\Omega \boldsymbol{\sigma}(\boldsymbol{w}_\varepsilon) : \boldsymbol{\epsilon}(\boldsymbol{w}_\varepsilon) d\Omega = -\int_\Omega \nabla \cdot \boldsymbol{\sigma}(\boldsymbol{w}_\varepsilon)\boldsymbol{w}_\varepsilon d\Omega.$$

According to Poincaré's inequality (see Lemma 2.1), we obtain that there exists a positive constant α such that

$$\|\boldsymbol{w}_\varepsilon\|_{L^2(\Omega)} \leqslant \alpha \Delta x \Delta y \sqrt{\Delta x^4 + \Delta y^4} \|D^3 \delta_\varepsilon\|_\infty \to 0, \quad \text{as } \Delta x, \Delta y \to 0,$$

where $D^3\delta_\varepsilon$ is the third derivative of Gaussian distribution. Hence, $\|\boldsymbol{w}_\varepsilon\| \to 0$, as $h \to 0$, which implies the convergence between u_ε and v_ε. □

3 Numerical Results

In this section, results in both one dimension and two dimensions are presented. Figure 3.1 shows the analytical solution of all three approaches from Eq (2.19), (2.20) and (2.21). The red and blue curves, which correspond to the Smoothed Delta approach and the Smoothed Particle approach, mostly overlapping regardless the choices of ε if we take the cell size is the same as ε. This indicates that the solutions to (BVP_S) and (BVP_{SP}) are consistent. As ε decreases, the solutions to the smoothed approach and the smoothed particle approach converge to the solution to the direct approach. In other words, Figure 3.1 confirms the consistency between all three approaches, as long as ε is efficiently small.

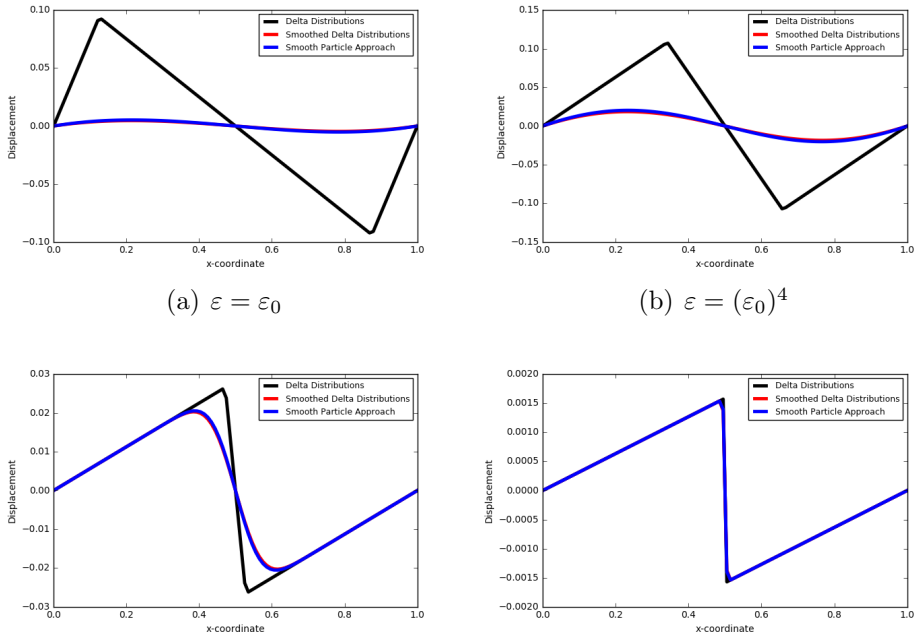

(a) $\varepsilon = \varepsilon_0$ (b) $\varepsilon = (\varepsilon_0)^4$

(c) $\varepsilon = (\varepsilon_0)^{10}$ (d) $\varepsilon = (\varepsilon_0)^{20}$

Figure 3.1: For one dimension, different colour of curves show the solution to (BVP_δ), (BVP_S) ***and*** (BVP_{SP}) ***respectively. Black curve shows the solution to the direct approach, red curve is the smoothed approach and blue curve is the smoothed particle approach. As*** $h = \varepsilon$ ***decreases, all the results converge***

For two dimensions, only the results applying Eq (2.4) will be shown. We consider only one big cell in the computational domain, and the boundary of the cell is split into finite line

segments. Based on the special case of square (see Eq (2.32) and Figure 2.1) and since the magnitude relation between the direct approach and the smoothed particle approaches is still unclear, we will use the area of the cell as the magnitude ratio. Subsequently, we will investigate the new cell area after deformation, as well as a region near the cell. Further, the computational time will be compared, since in our wound healing model, there are a large number of cells in the computational domain. In Figure 3.2, the bandwidth around the cell in the smoothed particle approach is wider than the direct approach, which is mainly because of the continuity of the smoothed particle approach. Table 3.1 displays the numerical results of the reduction in the volume of the vicinity region and the cell, as well as the computational cost. Using the cell volume as the ratio between the force magnitude in the direct and smoothed particle approach, the area results hardly show the discrepancy and the computational time is nearly the same. Therefore, considering the continuity property of the smoothed particle approach, it is promising to be collaborated in multiple cells model for the applications. On the other hand, we set the stiffness inside the cell close to zero, and the results are displayed in Table 3.2 and Figure 3.3. It is notable that the computation times, cell area reduction ratio and the vicinity area reduction are all more or less the same. Therefore, taking the advantage of a smooth force into consideration, the smoothed particle approach has the potential to be incorporated into the model containing multiple cells. In addition, compared with the Dirac Delta approach, the smoothed particle approach will not result in the singular solutions.

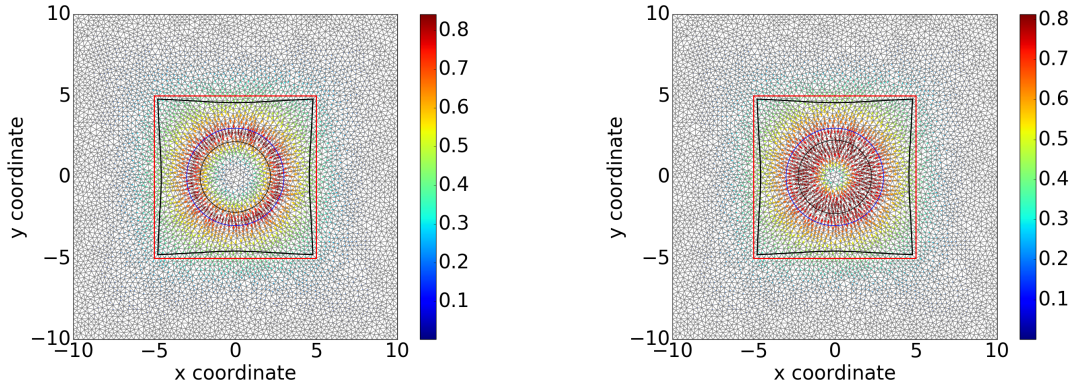

(a) Direct approach (b) Smoothed particle approach

Figure 3.2: For the constant stiffness of the computational domain, it is hard to see the difference between two subplots. Black curves show the deformed region of vicinity and the cell, and blue curve represents the cell

Table 3.1: The percentage of area change of cell and vicinity region, and time cost of the direct approach and the smoothed particle approach if the stiffness is constant over the computational domain

	Direct Approach	**Smoothed Particle Approach**
Cell Area Reduction Ratio(%)	47.81624	43.38118
Vicinity Area Reduction Ratio(%)	12.85195	12.88194
Time Cost(s)	1.70716	1.83455

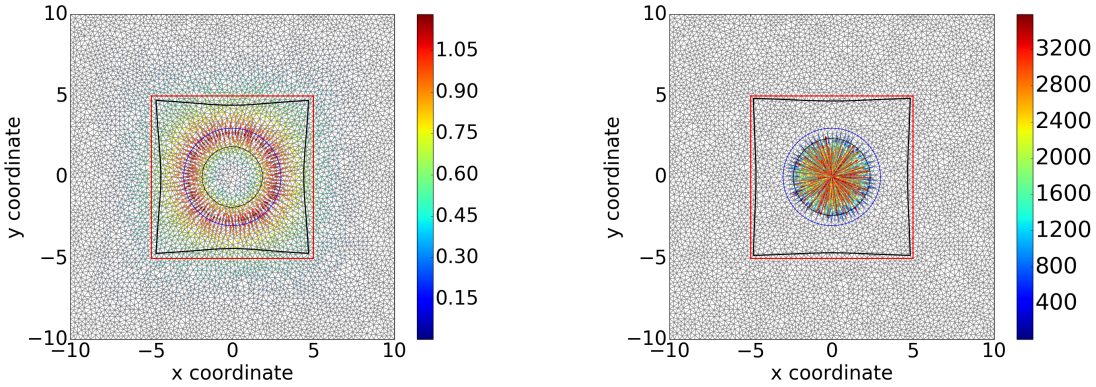

(a) Direct approach (b) Smoothed particle approach

Figure 3.3: For the different stiffness inside and outside of the cell, the magnitude of the displacement shows significant difference, but it is hard to see the differences on deformation between two approaches. Black curves show the deformed region of vicinity and the cell, and blue curve represents the cell.

Table 3.2: The percentage of area change of cell and vicinity region, and time cost of the direct approach and the smoothed particle approach when the stiffness inside and outside the cell differs

	Direct Approach	**Smoothed Particle Approach**
Cell Area Reduction Ratio(%)	61.92051	61.43349
Vicinity Area Reduction Ratio(%)	17.50153	17.48103
Time Cost(s)	1.99139	1.92355

4 Conclusion

In this paper, we developed two alternative methods using Gaussian distributions to replace Dirac Delta distribution in the point forces. The first method is the smoothed approach, in which the Dirac Delta distributions at the midpoint of boundary segments of the cell are replaced by Gaussian distributions directly. The second alternative method is the smoothed particle approach, which takes into account the gradient of the Gaussian distribution at the centre of the cell, and it is based on the point forces exerted on the boundary of cells in wound healing.

In one dimension, we proved that the smoothed approach and the smoothed particle approach converge to the direct approach, and the numerical results verified consistency. In two dimensions, we are not able to work out the exact ratio between the direct approach and the smoothed particle approach. However, inspired by the special case of square-shaped cell, we use the cell area to investigate the discrepancy, which turns out to be negligible. Furthermore, the smoothed particle approach costs nearly the same time as the direct approach, which offers the possibility to adapt it into the general healing model.

References

[1] B. D. Cumming, D. McElwain, and Z. Upton. A mathematical model of wound healing and subsequent scarring. Journal of The Royal Society Interface, 7(42):19–34, 2009.

[2] M. J. Eichler and M. A. Carlson. Modeling dermal granulation tissue with the linear

fibroblast-populated collagen matrix: a comparison with the round matrix model. Journal of dermatological science, 41(2):97–108, 2006.

[3] S. Enoch and D. J. Leaper. Basic science of wound healing. Surgery (Oxford), 26(2):31–37, 2008.

[4] E. Haertel, S. Werner, and M. Schäfer. Transcriptional regulation of wound inflammation. In Seminars in Immunology, volume 26, pages 321–328. Elsevier, 2014.

[5] D. Koppenol, C. Vuik, and P. van Zuijlen. Biomedical implications from mathematical models for the simulation of dermal wound healing. 2017.

[6] B. Laud. Electromagnetics. New Age International, 1987.

[7] B. Li and J. H.-C. Wang. Fibroblasts and myofibroblasts in wound healing: force generation and measurement. Journal of tissue viability, 20(4):108–120, 2011.

[8] F. Vermolen and A. Gefen. Semi-stochastic cell-level computational modelling of cellular forces: Application to contractures in burns and cyclic loading. Biomechanics and Modeling in Mechanobiology, 14(6):1181–1195, 2015.